Sub-wavelength imaging without metamaterials

Andrew J. Mackay
Q-par Steatite Antennas Ltd., UK
E-mail: andrew.mackay@q-par.com

***Abstract*—There is considerable interest in sub-wavelength imaging using metamaterials, for example using double negative isotropic materials or hyperbolic anisotropic materials. It is shown here that sub-wavelength imaging is possible using more conventional bulk isotropic materials with positive relative permeability ϵ_r and relative permittivity μ_r greater than unity. There are practical advantages to this approach. Firstly, such materials are inherently non-dispersive so that large bandwidths may be obtained. Secondly, conventional dielectric materials are available with low loss from radio to optical frequencies. Thirdly, difficult fabrication processes may be avoided. This letter provides examples using a magneto-electric material with $\epsilon_r = \mu_r$ in order to reduce interface reflections due to impedance mismatch while establishing proof of principal. The method uses a lens designed to ensure that rays in the medium, generated by evanescent modes near the source, are converted into free space propagating waves.**

***Index Terms*—metamaterials, super-resolution, superlens, imaging, ray tracing, evanescent waves**

I. Introduction

There have been many papers employing meta-materials to achieve sub-wavelength imaging where a source is imaged with a resolution smaller than $\lambda_0/2$ where λ_0 is the wavelength in the source medium [1]. A general requirement is the use of information in the evanescent fields near the source. Fields which are evanescent in the neighbourhood of the source are converted within the medium into propagating waves which can be accessed far from the source [2].

It is indicated here that it may be unnecessary to employ metamaterials. A conventional uniform thickness slab of high refractive index material will totally internally reflect waves beyond a certain critical angle and in the medium outside the slab these internally propagating waves are associated with external evanescent waves. If one surface of the slab is lensed it is possible for the evanescent-wave-sourced internally propagating waves to be converted into free space propagating waves. This method of accessing information contained within the evanescent fields provides a possible route to sub-wavelength imaging which does not rely on metamaterials.

From an alternative perspective a source close to an interface generates similar fields either side of the interface and in a high refractive index material the source spans more wavelengths as measured in the material so that imaging in the material resolves to of the order of $\lambda_n/2$ where $\lambda_n = \lambda_0/\sqrt{\epsilon_e \mu_e}$ and ϵ_e and μ_e are the effective relative permittivity and permeability at the interface, $1 < \epsilon_e < \epsilon_r$ and $1 < \mu_e < \mu_r$ with values expected to lie well away from the lower bounds.

II. Use of an ellipsoidal lens

There are advantages in employing a lens which converts all rays from a point source at the interface of one part of the lens to a family of parallel rays at the exit of the lens. A subset of these rays can be generated by evanescent fields. This is illustrated in fig. 1, below. In fact, this type of lens has been designed [3] for surface coupling to antennas. All that is necessary for the present purpose is that the refractive index should be sufficiently large to permit the conversion of evanescent fields into propagating waves. The lens is an ellipsoid of revolution with a cylindrical end section. The eccentricity of the ellipse, $e = 1/n$ where $n = \sqrt{\epsilon_r \mu_r}$ is the refractive index. It is assumed here that the lens is embedded in free space. This lens will be termed the evanescent field converter (EFC) lens. Following [3], the semi-minor and major

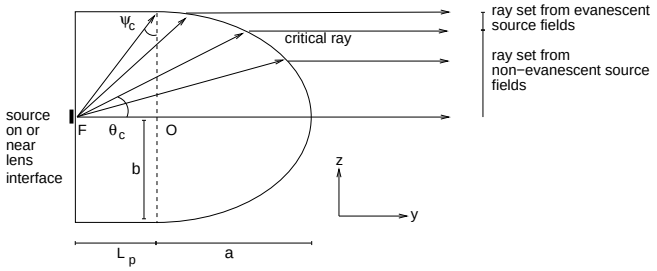

Fig. 1. Lensing from evanescent source fields using a non-meta-material

axis lengths are b and a and the distance from the origin O to the focal point F is $L_p = a.e$ where e is the eccentricity of the ellipse defined by $b^2 = a^2(1 - e^2)$. It is shown in [3] that $e = 1/n$ for parallel exit rays.

The critical ray angle θ_c within the EFC lens is given by $\theta_c = \arcsin(1/n)$. For angles $\theta > \theta_c$ within the lens, rays to the left of the lens are evanescent. Such internal propagating rays would be totally internally reflected if the rays could not escape through the curved surface of the lens. When the curve of the ellipse is parallel to the axis no further rays can be focused, under the ray approximation, so this defines a triangle where $\theta_c + \psi_c = \pi/2$ where ψ_c is the angle made by a ray with the end of the elliptical region (see fig. 1). The geometry shows that $\sin(\pi/2 - \psi_c) = \sqrt{(1 - e^2)} = \sqrt{(1 - 1/n^2)}$ and this must be greater than $\sin\theta_c = 1/n$. Consequently, for this lens structure, there is a limit placed on n given by $n > \sqrt{2}$ if super-resolution is to be achieved. In principle, the larger the value of n the larger the degree of super-resolution that should be possible since more internal rays are transmitted that convey shorter range evanescent field information. In practice, if n is too large there can be insufficient electrical matching of

the lens to free space, despite the employed (high frequency) match condition $\epsilon_r = \mu_r$.

III. A Numerical Example

In this example both sub-wavelength focusing and imaging capability is demonstrated. CST [4] is employed to simulate the fields generated by a small sub-wavelength dipole at three positions on the lens interface. The dipole consists of two thin conducting patches of length $\Delta z = 2.25$ mm and width $\Delta x = 2.5$ mm, in the z and x directions separated by a gap of constant width 0.5 mm fed with a 100 ohm line source. The two patches are thus bounded by a rectangle of size 5.0×2.5 mm parallel to the z-x plane. In one case the dipole is placed on axis at the lens interface flat side. In the others the dipole is offset by 5 mm and 10 mm in the z-direction. The dimension $b = 80.0$ mm is arbitrarily chosen, and a refractive index n is chosen such that (for good match conditions) $\epsilon_r = \mu_r = \epsilon_{el}$ so that $n = \epsilon_{el}$. Here, $\epsilon_{el} = 4.0$. Alternative matching techniques should be possible in order to use a more realistic material with $\mu_r = 1$, but these make the design more complicated. Possibilities include the use of quarter-wave matching layers on the curved lens boundaries but these will not be considered here.

It is possible to provide a demonstration with two EFC lenses back-to-back with a small space between or alternatively with the two EFC lenses separated by an additional two convex spherical imaging lenses. It is intended to generate a sub-wavelength image on the planar side of the second EFC lens where only radiated non-evanescent fields connect the two EFC lenses. In the first case, the image is inverted whereas in the second it is non-inverted. The second approach is preferred since the imaging lenses capture more of the radiated fields. It is expected that the degree of resolution is directly related to the cross-sectional area of the propagating field region but at present it is unclear how the evanescent wave information is encoded in the far-field so it is not known how to minimise the image distortion and maximise the resolution for a given EFC lens.

The imaging lens method employs two intermediate double spherical lenses. These latter lenses are also assumed to be well matched and made of a material with $\epsilon_r = \mu_r = \epsilon_{sp}$ and refractive index $n_{sp} = \epsilon_{sp}$. The intermediate imaging lenses are designed using the thick lens maker's formula,

$$\frac{1}{f} = (n_{sp} - 1)\left(\frac{2}{R} + \frac{(n_{sp} - 1)d}{n_{sp}R^2}\right) \qquad (1)$$

The focal point lies midway between the imaging lenses, i.e. they lie a distance $2f$ apart. R is the radius of curvature of both lenses and d is the thickness of the lenses along the lens axis. The geometry is symmetrical about the centre point of the system with the centre of the imaging lens nearest the source EFC lens a distance L_f from the origin O. This double spherical lens imaging system is not intended to be optimal, merely sufficient to demonstrate a super-resolution effect.

The focusing lenses are defined assuming $n_{sp} = 4.0$, $R = 800$ mm, $d = 30$ mm and $L_f = 428$ mm. The example frequency is 7 GHz where $\lambda_0/2 \approx 21.4$ mm. Fig. 2 shows the geometry with the previously defined source dipole centred on axis. The figure represents a colour magnitude plot with phase information generated by CST with non-offset source. The return loss from the source is poor at this frequency with $S11 \approx -2.5$ dB. This improves with increasing n, but is incidental to the demonstration. The field as shown is symmetrical about the x-y plane since the source lies on axis in this picture. However, it is not symmetrical about a plane parallel to the x-z plane, mid-way between the lenses. Such mid-point symmetry would be ideal since it would imply perfect reconstruction of the source fields. Unfortunately, this is not possible because the fields over the lenses lie over a region of space which is not electrically large and the incident fields are not represented by waves from a single location in space.

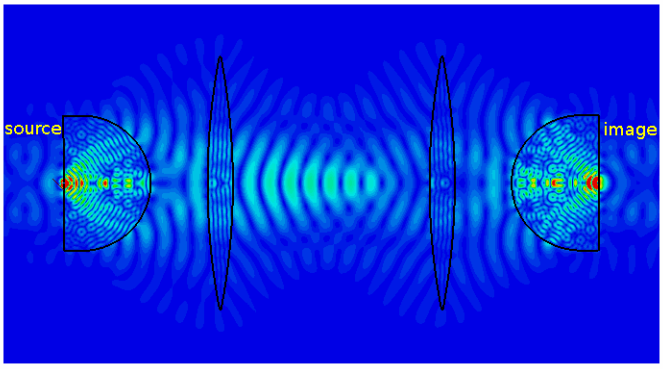

Fig. 2. Near fields in y-z plane showing EFC and intermediate lenses

Fig. 3 shows three plots of the field magnitude for the non-offset and offset source (5 mm and 10mm offsets in the z-direction) along a cut parallel to the z-axis for $x = 0$ in the image plane. The image plane is selected 0.5 mm behind the flat side of the EFC imaging lens (in free space) on the right hand side of fig. 2.

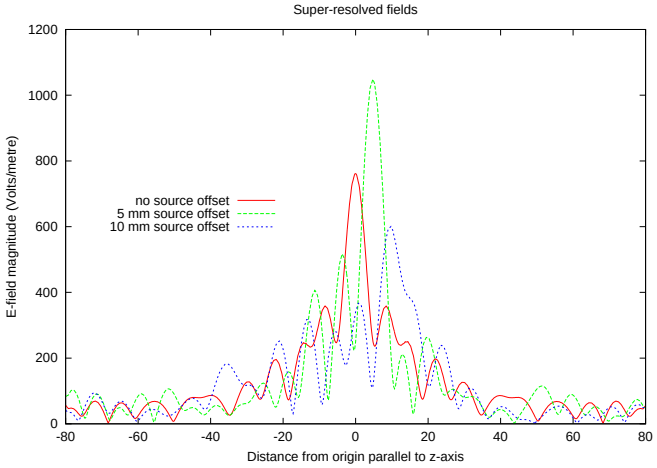

Fig. 3. Near field in the image plane, along a cut parallel to the z-axis

The result indicates a resolution of about 5 mm, which should be compared to $\lambda_0/2 \approx 21.4$ mm, so demonstrating a super-resolution factor of about 4.

IV. Conclusion

It is shown that a non meta-material lens can be used to image a sub-wavelength source with significant super-resolution. This establishes a proof-of-principal that meta-materials are not required for such purposes and consequently provides an alternative methodology that is likely to be insensitive to dispersion effects. Much work remains to understand how the far field encodes the super-resolved information and to devise better lensing systems if this is required. Ideally it would be desirable to reconstruct the image from far-field data without a refocus system, which was employed here principally to demonstrate that super-resolution information is contained in the free space propagating waves. It would also be interesting to investigate the use of a high dielectric constant non-magnetic material for EFC lens construction with quarter-wave matching layers on the curved surfaces. The author would welcome discussion on these matters.

Acknowledgements

This work has been part funded by Q-par Steatite antennas Ltd.

References

[1] A.M.H. Wong and G. V. Eleftheriades, "Advances in imaging beyond the diffraction limit", *IEEE Photonics Journal, Vol. 4, No. 2, pp 586-589, April 2012*.

[2] X. Zhang and Z. Liu, "Superlenses to overcome the diffraction limit ", *Nature Materials, Vol. 7, June 2008*. See www.nature.com/naturematerials.

[3] L. Mall, "Analysis into proximity-coupled microstrip antenna on dielectric lens", *Intech open science*, 2011, ISBN 978-953-307-247-0. See www.intechopen.com.

[4] CST studio suite, 2015. See www.cst.com.

Andrew Mackay received the Joint Hons B.Sc. in Mathematics and Physics from the University of Bristol, U.K., in 1981. He received a Ph.D. Degree in electrical engineering at the University of Swansea, U.K., in 1988. He worked at the Royal Signals and Radar Establishment (now part of QinetiQ), U.K., for about 14 years mostly on stealth technology and related research on materials and computational methods where he won the John Benjamin prize for work on FSS in 1989. He now works at Q-par Steatite Antennas as consultant and antenna designer. His interests include the growing of orchids and martial arts and currently holds a third dan black belt in Aikido.